Toxicology Letters 233 (2015) 187–199

Contents lists available at ScienceDirect

Toxicology Letters

journal homepage: www.elsevier.com/locate/toxlet

Changes in Caco-2 cells transcriptome profiles upon exposure to gold nanoparticles

Edyta Bajak [a,1], Marco Fabbri [a,b,1], Jessica Ponti [a], Sabrina Gioria [a], Isaac Ojea-Jiménez [a], Angelo Collotta [c], Valentina Mariani [a], Douglas Gilliland [a], François Rossi [a,*], Laura Gribaldo [d,**]

[a] European Commission, Joint Research Centre (JRC), Institute for Health and Consumer Protection (IHCP), Nanobiosciences (NBS) Unit, via E. Fermi 2749, 21027 Ispra (VA), Italy
[b] Department of Clinical and Experimental Medicine, University of Insubria, via J. Dunant, 5, 21100 Varese, Italy
[c] European Commission, JRC, IHCP, Molecular Biology and Genomics (MBG) Unit, via E. Fermi 2749, 21027 Ispra (VA), Italy
[d] European Commission, JRC, IHCP, Chemical Assessment and Testing (CAT) Unit, via E. Fermi 2749, 21027 Ispra (VA), Italy

HIGHLIGHTS

- Biological effects (toxicity, uptake and changes in gene expression patterns) on Caco-2 cells of citrate-stabilized 5 nm and 30 nm AuNPs were compared.
- Exposure to 5 nm AuNPs had much stronger effect on gene expression as compared to treatment with 30 nm AuNPs.
- Nrf2 signaling stress response was among the highly activated pathways.

ARTICLE INFO

Article history:
Received 22 August 2014
Received in revised form 10 December 2014
Accepted 12 December 2014
Available online 15 December 2014

Keywords:
AuNPs uptake
Stress responses
Cellular signaling
Transcriptomics
qPCR

ABSTRACT

Higher efficacy and safety of nano gold therapeutics require examination of cellular responses to gold nanoparticles (AuNPs). In this work we compared cellular uptake, cytotoxicity and RNA expression patterns induced in Caco-2 cells exposed to AuNP (5 and 30 nm). Cellular internalization was dose and time-dependent for both AuNPs. The toxicity was observed by colony forming efficiency (CFE) and not by Trypan blue assay, and exclusively for 5 nm AuNPs, starting at the concentration of 200 μM (24 and 72 h of exposure). The most pronounced changes in gene expression (Agilent microarrays) were detected at 72 h (300 μM) of exposure to AuNPs (5 nm). The biological processes affected by smaller AuNPs were: RNA/zinc ion/transition metal ion binding (decreased), cadmium/copper ion binding and glutathione metabolism (increased). Some Nrf2 responsive genes (several metallothioneins, HMOX, G6PD, OSGIN1 and GPX2) were highly up regulated. Members of the selenoproteins were also differentially expressed. Our findings indicate that exposure to high concentration of AuNPs (5 nm) induces metal exposure, oxidative stress signaling pathways, and might influence selenium homeostasis. Some of detected cellular responses might be explored as potential enhancers of anti-cancer properties of AuNPs based nanomedicines.

© 2015 The Authors. Published by Elsevier Ireland Ltd. This is an open access article under the CC BY license (http://creativecommons.org/licenses/by/4.0/).

1. Introduction

Nanotechnology and nanomedicine bring novel approaches into clinics, revolutionizing diagnosis and treatment options for diverse groups of patients. Engineered nanomaterials (ENMs) are also widely used in other consumer products and applications increasing the likelihood of human exposure to nanomaterials (Staggers et al., 2008). The exposure to ENMs can take place not only during their synthesis, production and usage, but also at other stages of the life cycle (*e.g.*, waste deposition/combustion, material

* Corresponding author. Fax: +39 0332 78 5787.
** Corresponding author. Fax: +39 0332 78 5707.
E-mail addresses: edyta.bajak@ec.europa.eu (E. Bajak), marco.fabbri@uninsubria.it (M. Fabbri), jessica.ponti@ec.europa.eu (J. Ponti), sabrina.gioria@ec.europa.eu (S. Gioria), isaac.ojea-jimenez@ec.europa.eu (I. Ojea-Jiménez), angelo.collotta@ec.europa.eu (A. Collotta), valentina.mariani@gmail.com (V. Mariani), douglas.gillland@ec.europa.eu (D. Gilliland), francois.rossi@jrc.ec.europa.eu (F. Rossi), laura.gribaldo@ec.europa.eu (L. Gribaldo).
[1] Contributed equally to this work.

http://dx.doi.org/10.1016/j.toxlet.2014.12.008
0378-4274/© 2015 The Authors. Published by Elsevier Ireland Ltd. This is an open access article under the CC BY license (http://creativecommons.org/licenses/by/4.0/).

recycling) of a given nanomaterial. Therefore, in order to assure the safety of human population and environment, toxicological profiling of cellular responses to ENMs and proper risk assessment of nanomaterials should be performed (Maynard, 2012). The (nano) toxicological hazard identification and characterization are also required for improvement of the safety and efficacy of nanomedicines, including nano gold based formulations used in biomedical applications. Moreover, studies focused on the consequences of the long-term exposures to ENMs, including gold nanoparticles (AuNPs), are needed (Kunzmann et al., 2011).

Gold belongs to the group of noble metals and has been used in medical applications for centuries (Bhattacharya and Mukherjee, 2008). In recent years, nano gold based applications were designed and AuNPs synthesized with the idea that noble metal characteristics (in bulk) of gold would be preserved even when synthesized and used at nano scale, thus being bio-compatible (Connor et al., 2005). AuNPs and their derivatives undergo continuous development for their use in clinical diagnostics, as drug delivery systems or therapeutic agents (Dykman and Khlebtsov, 2012). In general, AuNPs are well tolerated *in vivo* (Hainfeld et al., 2006), although some toxicity of AuNPs was also reported *in vitro* (Pernodet et al., 2006; Chuang et al., 2013; Coradeghini et al., 2013; Mironava et al., 2014).

As methodologies develop, "omics" based research platforms can complement the classical tools for cytotoxicity testing in (nano) toxicology field. Therefore, identification and characterization of biological responses can be achieved at molecular levels compromising biomarkers/endpoints that can include whole or parts of transcriptome, proteome, metabolome, epigenome and/or genome of the *in vitro*/*in vivo* system under investigation (Hamadeh et al., 2002). Although toxicogenomics and other "omics" methods are currently easily accessible and cost effective, to date only a few studies applied transcriptomics or proteomics tools in the study of AuNPs induced/mediated cellular responses (Esther et al., 2005; Yang et al., 2010; Li et al., 2011; Qu et al., 2013; Gioria et al., 2014).

All living organisms respond to diverse stress stimuli. Depending on the biological context of given exposure/stressor, its severity and duration, cells within tissue/organ react to stimuli by evoking stress or adaptation responses, or die (Fulda et al., 2010; Chovatiya and Medzhitov, 2014). One of the key regulators of cellular responses to endogenous and/or exogenous stress is the nuclear factor E2-related factor 2 (Nrf2) protein. Nrf2 is a redox and xenobiotics sensitive transcriptional factor, assuring the expression of proteins involved in cellular adaptation to oxidative stress, adjustment of metabolism and detoxification of drugs (Kensler et al., 2007). Under normal cellular conditions, Nrf2 functions as a tumor suppressor. However, it has been shown that Nrf2 might also act as an oncogene (Shelton and Jaiswal, 2013). Among gene targets regulated by Nrf2 are metallothioneins (MTs), which are small, cysteine rich and metal ion binding proteins. MTs play an important role in the protection of cells against metal toxicity, but are also involved in responses to oxidative stress, and exposure to glucocorticoids and cytokines (Miles et al., 2000).

The aim of this study was to investigate how the colorectal adenocarcinoma epithelial cell line (Caco-2), an *in vitro* model of the intestinal route of exposure to nanoparticles, responds to AuNPs treatments at RNA gene expression level. We selected undifferentiated cells mainly because in this way we looked at populations of heterogenic pool of Caco-2 cells prior to differentiation, therefore having wider plasticity in the cellular physiology, sensing and adaptation/response to stress, as compared to mature and polarized enterocytes (Tadiali et al., 2002). Keeping this in mind, when running both the cytotoxicity and RNA transcript profiling experiments, we explored Caco-2 cells (in undifferentiated stage) as potentially more suitable model for detecting alterations in gene expression patterns upon exposure to NPs. For that purpose, we tested citrate-stabilized spherical AuNPs of two sizes (5 nm and 30 nm, synthesized and characterized in-house) for their cytotoxic potential, internalization and induction of changes in mRNA and long non-coding RNAs expression patterns using transcriptomics approach (Agilent microarrays platform). The microarray data were further validated with quantitative real-time reverse-transcriptase PCR (qPCR) for a set of mRNAs which were differentially expressed upon exposure of Caco-2 cells to AuNPs. Several biological pathways affected by treatment of Caco-2 cells with AuNPs (5 nm, 300 μM, 72 h) were identified in microarray datasets using bioinformatical tools. The novelty of this work is the integration of classical *in vitro* testing with the chemico-physical characterization of NPs, Omics and advanced analytical techniques to better understand the mechanisms of potential nanomaterials' toxicity. Their use has the potential to provide a description of the bio-responses and allows highlighting critical biochemical pathways affected by nanoparticle exposure. Huge progresses have been made in the genomic field and here we integrated this discipline to investigate in detail modifications caused by AuNPs exposure at gene level. The results of this work established a starting point in understanding and disseminating which cellular processes can be linked to the observed cytotoxic effect of 5 nm AuNPs on cancer Caco-2 cells.

2. Materials and methods

2.1. AuNPs synthesis and characterization

AuNPs of approximately 5 nm and 30 nm size in diameter were synthesized and concentrated as described in literature (Coradeghini et al., 2013; Turkevich et al., 1951). Detailed description of the chemicals used for AuNPs synthesis, description of the equipment used for particles size distribution and characterization, sample preparation, image acquisition and processing, can be found in Supplementary methods.

The stability of AuNPs dispersions was studied both using a centrifugal particle sedimentation (CPS) instrument and by zeta-potential measurements in representative media. Citrate-stabilized AuNPs (5 and 30 nm) were incubated at two different concentrations (100 and 300 μM) in three different media (milliQ-water, serum-free cell culture medium and complete cell culture medium). Measurements were made immediately after mixing AuNPs samples with the corresponding medium (time 0) and then again after 24 and 72 h incubation times at 37 °C.

AuNPs dispersions for cell exposure experiments were freshly prepared by diluting the AuNPs suspensions (after concentration step, as described in the Supplementary methods) in complete culture medium, and were added directly to Caco-2 cell cultures. The concentration step produced two solutions containing all the reagents used for the NPs synthesis and they were used as solvent controls for biological testing.

2.2. Cell culture

Human epithelial colorectal adenocarcinoma cells (Caco-2) are from the European collection of cell cultures (ECACC) and were purchased from Sigma (Catalogue number: 86010202; passage 45). Experimental cultures were prepared from deep-frozen stock vials and maintained in a sub-confluent state. They were grown in complete cell culture medium composed of high glucose (4.5 g/mL) Dulbecco's modified Eagle medium (DMEM), supplemented with 10% (v/v) fetal bovine serum (FBS), 4 mM L-glutamine and 1% (v/v) pen/strep (all from Invitrogen, Italy). Cultures were maintained in cell culture incubator (HERAEUS, Germany) under standard culture conditions (37 °C, 5% CO_2 and 95% humidity). Caco-2 cells used in

this work were screened for the presence of *Mycoplasma* with quantitative PCR (qPCR) using the Venor®GeM Prime kit and were *Mycoplasma* free.

2.3. Cytotoxicity assays

Cytotoxic effect of AuNPs in Caco-2 cells was studied by colony forming efficiency (CFE) and Trypan blue exclusion assays.

For the CFE, cells were seeded at the density of 200 cells per 60 × 15 mm dish (Corning, Italy) in 3 mL complete culture medium (three replicates) for each treatment. Twenty four hours after plating, the medium was changed and 3 mL of fresh medium containing the AuNPs was added to obtain the final AuNP concentrations of 10, 50, 100, 200 and 300 μM corresponding to 0.02, 9.85, 19.70, 39.40 and 59.10 μg/mL, respectively. After 24 and 72 h of exposure, the medium was replaced with fresh complete culture medium. On the 13th day from seeding, cells were fixed with 3.7% (v/v) formaldehyde solution (Sigma–Aldrich, Italy) in phosphate-buffered saline (PBS) without calcium, magnesium and sodium bicarbonate (Invitrogen, Italy) and stained with 10% (v/v) Giemsa GS-500 solution (Sigma–Aldrich) in ultra pure water. Solvent controls (cells exposed to two different solvents obtained after AuNPs of 5 nm and 30 nm filtration, as used for the highest concentration tested) and a positive control (1 mM) sodium meta chromate (Sigma–Aldrich) were included. Colonies were scored using a cell colony counter GelCount (Oxford Optronix Ltd., UK).

For Trypan blue exclusion assay, 2.5×10^5 and 0.9×10^5 cells were seeded for 24 h and 72 h exposures, respectively, in 6 well plates (Falcon, Italy) with 2 mL of complete cell culture medium. Twenty four hours after plating, cells were exposed to 50, 100 and 300 μM of 5 and 30 nm AuNPs, corresponding to 9.85, 19.70, and 59.10 μg/mL. At the end of the exposure time (24 or 72 h), cells were washed twice with PBS, detached with 0.5 mL of 0.05% trypsin sodium ethylene diamine tetraacetic acid (Trypsin-EDTA) from Invitrogen, and harvested with 1 mL of complete culture medium. Next, 30 μL of each sample was stained with 30 μL of Trypan Blue (Sigma–Aldrich) and cells were counted with the TC10 automated cell counter (Biorad, Italy) according to the supplier's protocol. Negative control, solvent control and positive control were also included in the test, as described for CFE assay.

In the CFE and Trypan blue assays, the results were normalized to the solvent control. For the CFE assay, they are expressed as CFE (%) ([average number of treatment colonies/average number of solvent control colonies] × 100). For the Trypan blue assay, they are expressed as viability (%) ([number of cells in treatment/number of cells in solvent control] × 100). One-way analysis of variance (ANOVA) with *post-hoc* test (Dunnett's multiple comparison test) for comparing groups of data against one control group was used. Data are reported as mean values ±SEM (standard error mean = standard deviation/√number of replicates). The data represents mean value of three independent biological replicas, where p values of less than 0.05 (*) and 0.001 (***) were considered statistically significant. Statistical calculations were carried out using GraphPad Prism Version 5.0 (GraphPad Software, USA).

2.4. Nanoparticle internalization

The uptake of AuNPs, their association with cellular membrane/matrix and internalization were quantified by Inductively Coupled Plasma Mass Spectrometry (ICP-MS). The uptake of AuNPs, association of AuNPs with cellular membrane/matrix and the internalization of AuNPs was quantified by ICP-MS. For the ICP-MS, 7×10^5 and 3×10^5 CaCo-2 cells were seeded in dishes from Corning (100 mm × 15 mm) for 24 and 72 h exposure time respectively, in 5 mL of complete culture medium. Twenty four hours after seeding, cells were treated for 24 and 72 h with 5 and 30 nm AuNPs (100 and 300 μM). At the end of the exposure time, the medium was removed and collected for each sample, cells were washed twice with PBS and each wash collected in a separate tube. Cells were then detached with 1 mL of Trypsin-EDTA (Invitrogen, Italy) and harvested with 5 mL of complete culture medium. After this, cells suspension was centrifuged at 200 × g for 5 min (4 °C), and the supernatant was transferred into a new tube. The cellular pellet was suspended in 1 mL of culture medium. An aliquot of each sample (20 μL) was taken for cell count with TC10 automated counter. The total content of Au in the cells (cellular pellet) as well as in all the fractions collected from each cell culture sample: (i) medium at the end of the treatment (24 and 72 h), (ii) supernatants from the two washes, (iii) cellular pellet, and (iv) the final supernatant (representing a third wash), were analyzed by ICP-MS after mineralization with Aqua Regia (HNO_3:HCl at 1:3 ratio) and microwave digestion (2 cycles at 950 W for 10 min) in a Discover-Explorer microwave instrument (CEM Corporation, USA). These extensive washing of cells and sample collection steps for Au content measurements were applied to remove weakly bound AuNPs and to assure that the total starting amount of Au given to the cells was recovered among different fractions (including both, strongly associated with and/or internalized by cells and not taken up by cells). Three independent experimental replicas were carried out and the results were expressed as pg Au/cell, % of the external exposure concentration and as a number of NPs/cell. Calculations were performed as described in Coradeghini et al. (2013).

2.5. Exposures to AuNPs and RNA extraction

For the gene expression experiments, 2.5×10^5 and 0.9×10^5 Caco-2 cells were seeded in 2 mL complete cell culture medium, in a 6 well/plate (Falcon, Italy), and incubated for 24 and 72 h with 5 nm or 30 nm AuNPs, at either 100 and 300 μM concentrations. At the end of the treatment, the exposure medium was removed and cells were washed twice with PBS, and harvested with 300 μL of RLT plus RNeasy lysis buffer (Qiagen, USA). Cell lysates were collected from wells and stored at −80 °C until the RNA extraction step was performed. The details of RNA isolation are available in Supplementary methods.

2.6. Microarray expression profiling

The microarray (Agilent Whole Human Genome Oligo Microarray: 4 × 44 k 60 mer slide format) experiments were designed to perform three biological replicates for each time point (24 and 72 h), AuNPs size (5 and 30 nm) and concentration (100 and 300 μM) with complete medium and solvent controls. All the cRNA synthesis/sample-labeling, hybridization, washing, and scanning steps were conducted following the manufacturer's specifications (Agilent Technologies Inc., USA). Procedures for microarrays based data generation are described in Supplementary methods.

2.7. Quantitative PCR validation of microarray data

A real-time quantitative PCR (qPCR) analysis has been done on the same RNA samples that were used for the microarray hybridization, with the aim to validate the microarray results. All reagents for the qPCR and equipment were from Applied Biosystems, USA. The details of qPCR validation process and data analysis using delta–delta Ct method (Livak and Schmittgen, 2001) are available in Supplementary methods.

2.8. Gene expression data analysis

Quality control and array normalization were performed in the *R* statistical environment using the Agi4x44PreProcess (v 1.18.0)

package, downloaded from the Bioconductor web site (Gentleman et al., 2004). The normalization and filtering steps were based on those described in the Agi4x44PreProcess reference manual. Briefly, Agi4x44PreProcess options were set to use the mean signal and the BG median signal as foreground and background signals, respectively. Data were normalized between arrays by the quantile method (Bolstad et al., 2003). In this approach, the distribution of intensities of different microarray chips are transformed to become equal so that intensities can be compared between each other. In order to detect expression changes among different treatment conditions, the moderated *t* test was applied. Moderated *t* statistics were generated by Limma Bioconductor package. Modulated genes were chosen as those with a fold change greater than 1.5 $\log_2$ fold change and a false discovery rate (Benjamini and Hochberg's method) corrected *p*-value smaller than 0.05 (Smyth, 2004). Microarray results have been submitted to NCBI's gene expression omnibus (GEO) repository and are available under accession number GSE55349.

2.9. Bioinformatics

Up regulated and down regulated genes were analyzed in the Kyoto Encyclopedia of Genes and Genomes (KEGG) database (http://www.genome.jp/kegg/) in order to identify genes with similar functions. Expression analysis systematic explorer (EASE) biological theme analysis was conducted online using DAVID bioinformatics resources server (http//david.abcc.ncifcrf.gov/). Phylogenetic tree creation (rVISTA), co-expression network visualization (FunCoup) and *in silico* miRNA binding sites prediction (DIANA-mirExTra) are described in Supplementary methods (Alexeyenko et al., 2011; Alexiou et al., 2010; Dubchak et al., 2013).

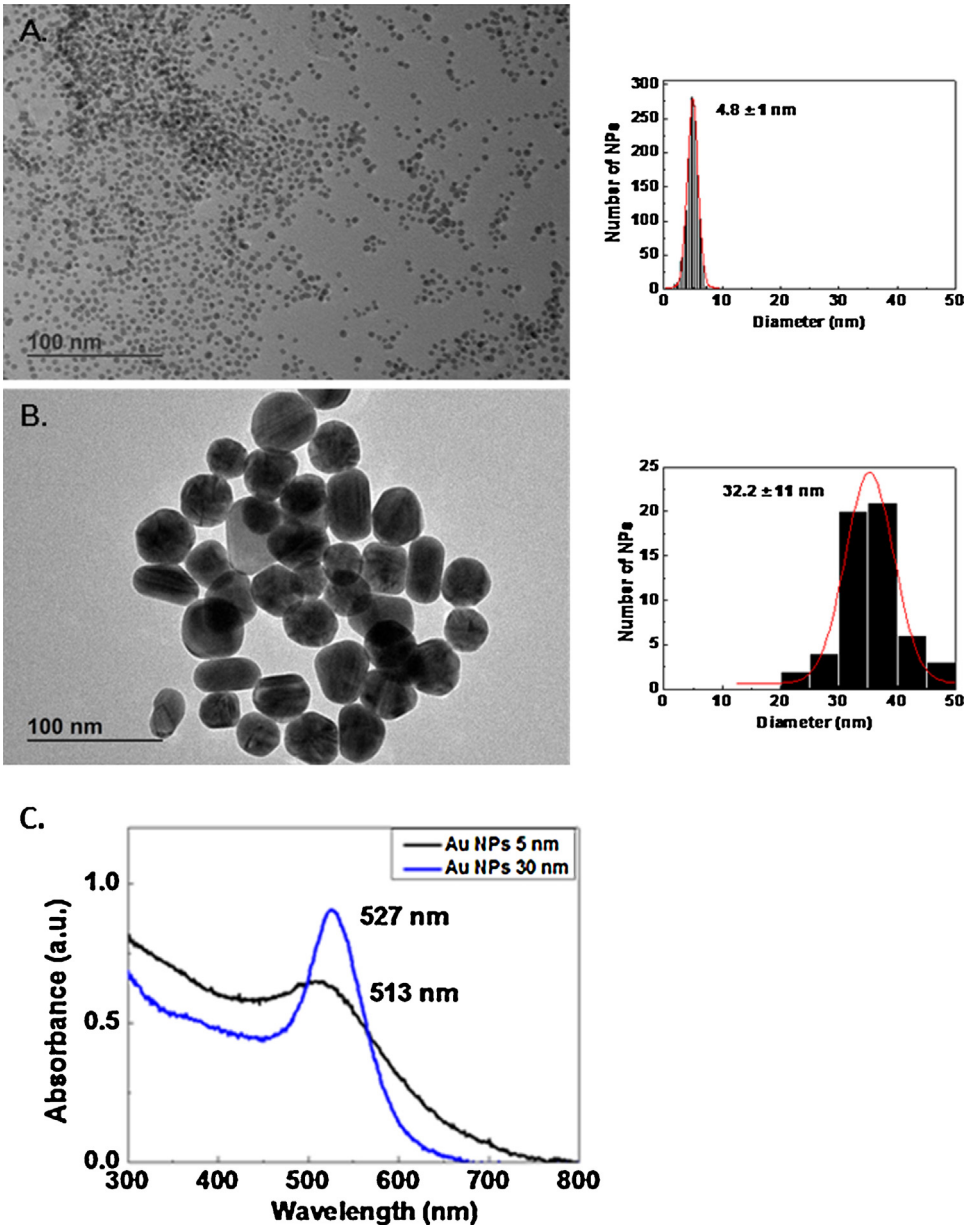

Fig. 1. Transmission electron microscopy (TEM) images and UV–vis absorption spectra of AuNPs. Morphology and size distributions of citrate-stabilized AuNPs of 5 nm (A) and 30 nm (B) in diameter. The histograms show size distributions of given AuNPs size, estimated with ImageJ software. UV–vis absorption spectra (C) of 5 nm AuNPs (black line) and 30 nm AuNPs (blue line). (For interpretation of the references to color in this figure legend, the reader is referred to the web version of this article.)

Table 1
Mean size distribution of AuNPs as measured by centrifugal sedimentation (CPS). Mean sizes of AuNPs samples (5 and 30 nm) incubated in water, Caco-2 cell culture medium without and with 10% (v/v) serum for 0, 24 and 72 h. Incubations took place in a cell culture incubator (in the dark). Abbreviations – HW: half width; PdI: polydispersity index; nd: not determined.

AuNPs	Au conc. (μM)	Mean size in water (nm) HW/PdI			Mean size in serum free cell medium (nm) HW/PdI			Mean size in cell medium with serum (nm) HW/PdI		
Sampling time		0 h	24 h	72 h	0 h	24 h	72 h	0 h	24 h	72 h
AuNPs 5 nm	100	3.9	4.1	4.5	41.0	52.2	47.3	5.5	4.5	4.4
		1.4/1.9	1.5/1.8	nd/1.8	21.5/1.2	26.0/1.2	23.7/1.2	nd/5.1	5.2/2.7	5.6/2.6
	300	3.9	4.0	4.5	51.1	53.8	50.5	4.9	5.5	5.5
		1.7/1.3	1.6/1.3	2.0/1.3	28.3/1.2	27.2/1.2	25.3/1.2	nd/2.6	5.2/1.6	4.9/1.9
AuNPs 30 nm	100	22.5	30.4	30.3	56.7	105.1	101.1	23.2	21.8	21.5
		6.4/1.3	6.7/1.1	6.4/1.1	26.2/1.3	64.4/1.4	57.8/7.0	6.6/1.4	6.4/1.3	6.3/1.3
	300	30.8	30.2	30.7	63.1	109.3	103.1	22.7	22.6	22.5
		6.0/1.1	6.3/1.1	5.9/1.1	41.6/1.4	73.7/1.5	81.4/1.6	7.0/1.3	5.9/1.2	5.8/1.4

3. Results

3.1. Characterization of AuNPs

Fig. 1A and B shows representative TEM images of the two nano gold samples used in this study. The morphologies observed were mainly spherical, although for 30 nm AuNPs it could also be observed a certain degree of faceting. Size distributions determined by TEM image analysis were narrow 4.8 ± 1.0 and 32.2 ± 11.0 nm, and the absorption band maximum measured by UV–vis spectrometry were in agreement with expected diameters of 5 nm and 30 nm AuNPs (Fig. 1C). It has been shown that the position of the surface plasmon resonance peak of Au NPs can be used to determine both size and concentration of gold nanoparticles (Haiss et al., 2007). Dynamic light scattering size measurements were also in agreement with the rest of characterization techniques (Suppl. Fig. 1) showing a mean size distribution, expressed as intensity (%), of 7.5 nm and 37.3 nm for 5 nm and 30 nm AuNPs, respectively.

Disc centrifuge sedimentation analysis using CPS technology was considered as an appropriate technique to monitor and measure the size distributions of AuNPs suspension samples in water, culture medium without serum and in complete cell culture medium, supplemented with 10% of serum (Table 1). The particles size distributions in water when measured by CPS are in agreement with those determined by TEM image analysis. As expected, in the absence of serum in cell medium, AuNPs aggregated, showing increase in AuNPs diameters. Aggregation was more noticeable at higher concentrations and for longer incubation times. However, in complete cell medium supplemented with serum proteins, no aggregation was observed and the NPs size was slightly larger to the one obtained in water due to the formation of a protein corona.

Zeta-potential measurements (Suppl. Fig. 2) were also performed in order to determine the evolution of the AuNP surface charge after incubation in cell culture media (with or without serum) and in water. Zeta-potential of AuNPs showed initial values between −30 and −40 mV in water. After incubation with cell culture medium in the presence of serum proteins, for both sizes (5 and 30 nm) and concentrations (100 and 300 μM) of AuNPs, a sudden change of the negative value of zeta-potential already occurring after mixing (time 0), is observed. At longer incubation times, zeta-potential values evolved toward the average charge of serum proteins (zeta-potential about −13.5 mV in our experimental system), which is indicative of the absorption of proteins at the surface of the NPs.

Finally, the concentration of ions released from the AuNPs suspensions, when measured by ICP-MS for up to 72 h in complete culture medium, was for both sizes of AuNPs below the detection limit of the technique (<1 ppb).

3.2. Cytotoxicity

Nano gold cytotoxicity in Caco-2 cells was evaluated using two methods: CFE assay and Trypan blue exclusion assay. The CFE is a standard test, already optimized for studying the toxicity of NPs (Ponti et al., 2010) and which is undergoing an inter-laboratory comparison of performance and reproducibility testing in the frame of the OECD working party of manufactured nanomaterials (work in progress). Cells were exposed to 5 and 30 nm AuNPs for 24 and 72 h, at concentrations ranging from 10 to 300 μM, as described in Supplementary methods.

Statistically significant cytotoxicity was observed only for 5 nm AuNPs when tested by CFE (Fig. 2A and B). Under the same exposure conditions, small decrease in cell viability at 100 and 300 μM was detected by Trypan blue assay. Although the observed drop in the membrane integrity was statistically not significant (Fig. 2C and D), its biological effects as a results of exposure of Caco-2 cells to 5 nm AuNPs, in particular to the highest concentration tested (300 μM), were evident when looking at detected changes in gene expression patterns. Interestingly, the cytotoxicity end-points based on changes in the membrane permeability detected by Trypan blue assay or efficiency in colony formation observed in CFE, were not statistically significant in Caco-2 cells exposed to 30 nm AuNPs, even for the highest concentration (300 μM) and at the longest (72 h) exposure time tested (Fig. 2). No significant difference in the number of colonies scored in the negative controls was observed in comparison to the solvent controls. As expected, for both *in vitro* cytotoxicity assays, treatment of Caco-2 cells with 1 mM sodium meta chromate (positive control) resulted in complete cell death (data not shown).

3.3. Nanoparticles internalization

The interaction of 5 and 30 nm AuNPs with Caco-2 cells was studied and quantified by ICP-MS after exposure to 100 and 300 μM nano gold suspensions (Fig. 3).

Internalization of gold in Caco-2 cells is expressed as pg/cell of Au, as % of Au *vs* total or number of NPs/cell. After 24 and 72 h of exposure at both 100 or 300 μM of Au 5 nm, cells incorporated approximately the same amount of Au; while we observed a dose-dependent increase of the Au 30 nm internalisation after both 24 and 72 h of exposure (Fig. 3A).

Interestingly, when the results are expressed as % of Au *vs* total exposure, for both AuNPs 5 and 30 nm a time-dependent increase in cell interaction and uptake was observed (Fig. 3B); and when expressing the data as a number of NPs in each cell the internalization of AuNPs 5 nm seems to be more efficient as compared to AuNPs 30 nm and no dose or time-dependent uptake manner was observed (Fig. 3C).

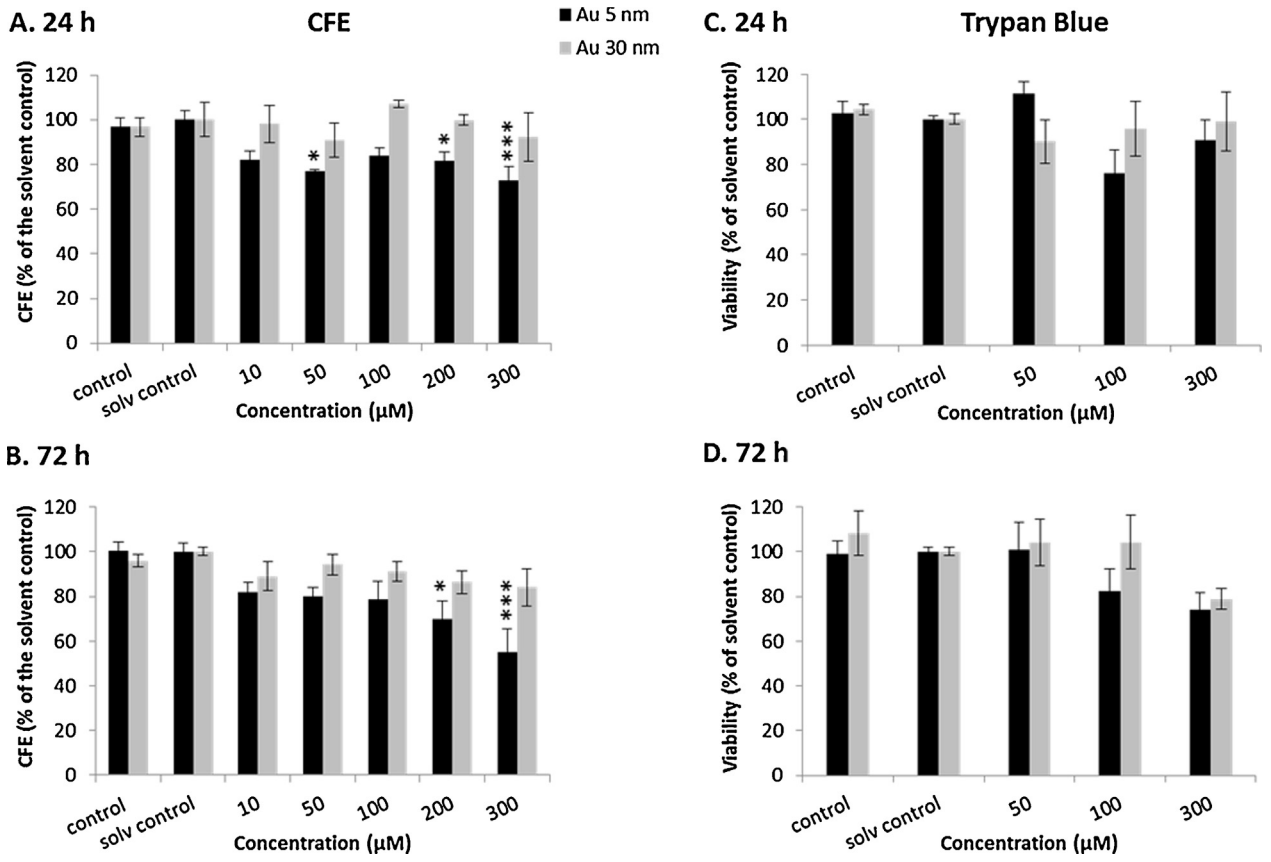

Fig. 2. Cytotoxic effects of 5 nm and 30 nm AuNPs on Caco-2 cells. The cytotoxicity of 5 nm AuNPs (black bars) and 30 nm AuNPs (gray bars) were estimated by colony forming efficiency (CFE) and Trypan blue exclusion assays. CFE assay: Caco-2 cells were exposed to increasing concentrations (10–300 μM) of AuNPs for 24 (A) and 72 h (B). In this range of concentrations and time points tested, no cytotoxicity was found in Caco-2 cells exposed to 30 nm AuNPs; while statistically significant cytotoxicity was observed for 5 nm AuNPs after 24 and 72 h of exposure to 200 μM ($^{*}p < 0.05$) and 300 μM ($^{***}p < 0.001$). Trypan blue exclusion assay: cell viability was tested on Caco-2 cells exposed for 24 (C) and 72 h (D) to increasing concentrations of 5 and 30 nm AuNPs (50–300 μM). Results of both assays represent a mean of three independent experiments (three replicates each) ± standard error of the mean (SEM) and are expressed in (A) and (B) as CFE (% of solvent control), while in (C) and (D) as viability (% of solvent control), respectively.

3.4. Gene expression profiling

As the major goal of our work was to get a better understanding of which molecular pathways might be affected by gold nanoparticles, we investigated the gene expression profiles of Caco-2 cells treated for 24 and 72 h with 5 and 30 nm nano gold, at two concentrations (100 and 300 μM), and compared them with the RNA transcripts levels of untreated cells (negative control).

First, a comparison of gene expression in cells treated with solvent (solvent control) *vs* the negative control was run and since almost no change was observed in the solvent control of Caco-2 cells (data not shown), we used untreated cells as reference control for gene expression profiling experiments. Thereafter, an induction or repression greater than 1.5 $\log_2$ fold change (that corresponds to an increase/decrease of 50%) and with a false discovery rate (FDR) corrected *p* value smaller than 0.05, were used to compare control data sets *vs* different treatment conditions for AuNPs exposures.

At the lower concentration of AuNPs (100 μM), a minimal number of differentially expressed genes was found. There were no gene transcripts that were regulated by the 5 nm AuNPs neither at 24 nor at 72 h. However, there were four mRNAs induced in Caco-2

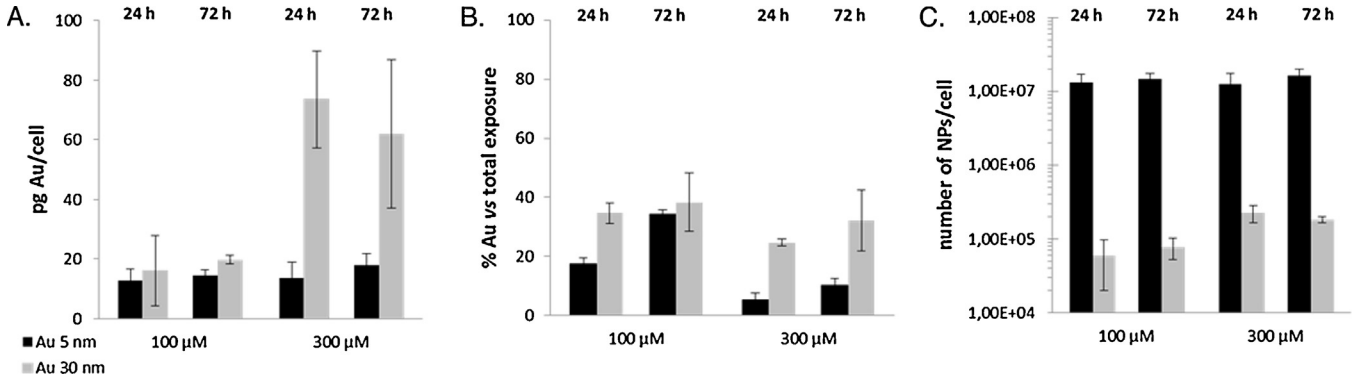

Fig. 3. Internalization of AuNPs by Caco-2 cells. The AuNPs cell interaction and uptake were measured by ICP-MS in Caco-2 cells incubated in the presence of 5 and 30 nm AuNPs (100 and 300 μM) for 24 and 72 h. Data are reported as pg Au/cell (A), % of Au in respect to the total Au exposure (B), and number of AuNPs/cell (C).

cells exposed to 30 nm nano gold (100 μM) after 24 h, and none of these genes was further affected after 72 h (Fig. 4A). Among these genes which mRNAs are increased, we find neurotensin receptor 2 (NTSR2) and two zinc finger containing transcriptional factors: human immunodeficiency virus type I enhancer binding protein 2 (HIVEP2) and zinc finger, DHHC-type containing 11 protein (ZDHHC11) involved in palmitoylation of proteins (Evers, 2006; Fukuda et al., 2002; Oku et al., 2013). Moreover, a gene locus LOC644662, which encodes yet uncharacterized novel long intergenic non-coding RNA (Zhang et al., 2011) was induced by 30 nm AuNPs (100 μM, 24 h).

At the highest AuNPs concentration tested (300 μM), a clear effect on gene expression can be observed, especially in 5 nm AuNPs treated Caco-2 cells. Here, at the earlier time point (24 h), we were able to detect 177 regulated genes (all down regulated). At the later time point (72 h) 811 transcripts were differentially expressed, with 103 up and 708 being down regulated. We observed a large fraction of genes which were down regulated already at 24 h (163), with their mRNAs levels being also decreased at 72 h (Fig. 4B).

Among the mRNAs highly up regulated upon exposure of Caco-2 cells to 5 nm AuNPs (300 μM, 72 h), were found the RNA transcripts of seven members of the methallothionein (MT) family genes, as well as genes of heme oxigenase (decycling) 1 (HMOX1), gastrointestinal glutathione peroxidase 2 (GPX2) and glucose-6-phosphate dehydrogenase (G6PD). Interestingly, already at 24 h time point of 5 nm AuNPs treatment (300 μM), the decrease of two selenoproteins' mRNAs (SELT and 15 kDa selenoprotein) was detected. A further decrease of SELT and 15 kDa selenoprotein expression levels, as well as mRNAs of two other selenoproteins (SELK and SEPP1) was observed at 72 h after exposure to 5 nm nano gold.

Under the same treatment conditions (300 μM) exposure of Caco-2 cells to larger AuNPs (30 nm) had no or very limited effects on gene expression patterns. For example, after 24 h we could not detect changes in RNA transcripts levels, and only four transcripts were detected as down regulated 72 h after treatment. The RNA transcripts of the following genes were altered in response to 30 nm AuNPs exposure: cadherin 16 (CDH16), carboxypeptidase A2 (CPA2), TSC22 domain family, member 3 protein (TSC22D3) and cysteine-rich PAK1 inhibitor (CRIPAK). The CDH16 gene product is a member of the cadherin family of cell adhesion, calcium dependent, membrane associated glycoproteins. Another mRNA induced by larger in size nano gold particle tested (30 nm), is a gene product of CPA2, which encodes a secreted protein involved in catabolic and digestion processes of other proteins (Vendrell et al., 2000). The third differentially expressed gene TSC22D3 encodes a leucine zipper transcription factor. Several studies showed that TSC22D3 gene, also known as GLIZ/DIP/TSC-22R, is induced by glucocorticoids (GCs), and plays a very important role as mediator in the anti-inflammatory and immunosuppressive action of GCs (Ayroldi and Riccardi, 2009). The fourth up regulated gene, CRIPAK is a novel endogenous inhibitor of p21-activated protein kinase 1 (Pak1). This kinase plays an important role in cytoskeleton organization, promotion of the cell survival responses and estrogen receptor (ER) mediated signaling (Talukder et al., 2006). Among these four genes, the mRNA of TSC22D gene was also down regulated in response to 5 nm AuNPs exposure (300 μM, 72 h). Thus, the other three genes (CDH16, CPA2, CIRPAK) showed decrease in their corresponding mRNAs levels only when the Caco-2 cells were treated with 30 nm nano gold particles.

3.5. Validation of microarray data with PCR

A subset of genes identified during microarray profiling was chosen for validation with real-time quantitative PCR (qPCR). The target selection of mRNAs (12 targets) for validation study was based on manual screening of differentially expressed genes, with

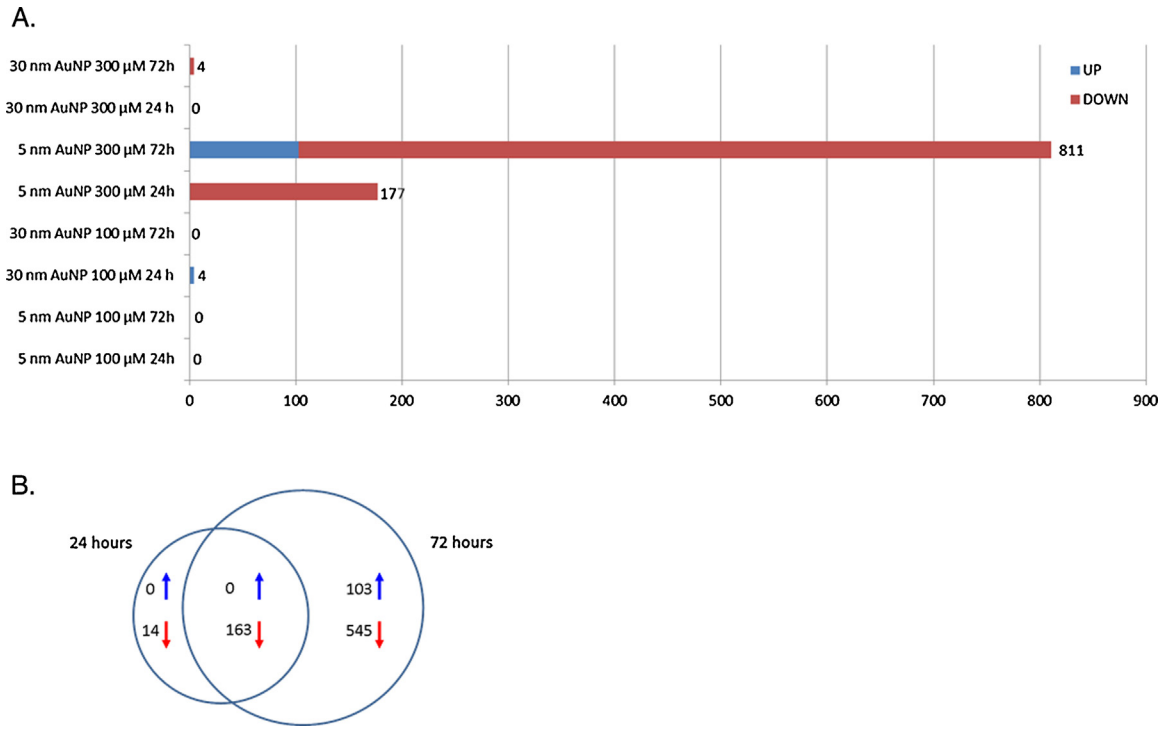

Fig. 4. Differentially expressed genes in Caco-2 cells exposed to 5 and 30 nm AuNPs. The bar graph (A) shows numbers of differentially expressed genes across RNA transcripts present on Agilent Whole Human Genome Oligo Microarray (4 × 44 k 60 mer slide format) and which were up and down regulated in Caco-2 cells as result of diverse exposure conditions to AuNPs. The Venn diagram (B) represents shared and time-specific numbers of genes regulated at 24 and 72 h after exposure to 5 nm AuNPs (300 μM).

Table 2
Validation of selected mRNAs with qPCR. Fold change expresses the difference of the mean log control and mean log stimulated data. Genes identified as regulated (log 2 fold greater than 1.5 and with false discovery rate (FDR) corrected *p* value smaller than 0.05) are coloured in red (down regulated) and blue (up regulated). The cells in the table are coloured in gray, when log 2 fold change is greater than 1.5 but the *p* value is not significant.

Gene symbol	QPCR				Microarray			
	5 nm AuNP 100 μM 24 h	5 nm AuNP 100 μM 72 h	5 nm AuNP 300 μM 24 h	5 nm AuNP 300 μM 72 h	5 nm AuNP 100 μM 24 h	5 nm AuNP 100 μM 72 h	5 nm AuNP 300 μM 24 h	5 nm AuNP 300 μM 72 h
ATF1	−0.21	−0.22	−0.86	−0.86	−0.28	−0.56	−0.87	−1.31
BIRC2	−0.54	−0.64	−1.06	−1.17	−0.32	−0.44	−0.98	−1.10
C1D	−0.43	−0.46	−1.09	−1.13	−0.46	−0.63	−0.95	−1.28
DNAJC21	−0.24	0.09	−0.43	−0.15	−0.18	−0.35	−0.22	−0.63
GPX2	−0.20	0.17	0.37	1.19	0.18	0.47	0.31	0.91
HAT1	−0.51	−0.64	−0.55	−0.55	−0.26	−0.49	−0.44	−0.76
HMOX1	0.00	0.36	0.36	1.82	0.16	0.39	0.29	1.42
MT2A	−1.32	0.30	0.48	3.95	0.15	1.94	0.30	3.55
OSGIN1	−0.07	−0.21	0.32	0.85	0.23	0.29	0.27	0.64
POLK	−0.17	−0.10	−0.82	−0.68	−0.48	−0.26	−0.67	−0.73
SRSF10	−0.17	−0.21	−0.66	−0.52	−0.26	−0.35	−0.61	−0.70
UBA2	−0.11	−0.02	−0.59	−0.40	−0.14	−0.18	−0.61	−0.52

an aim to select mRNAs covering diverse biological and biochemical functions which might be altered in Caco-2 cells when exposed to AuNPs.

Several members of genes involved in responses to oxidative stress, metal exposure and changes in cellular redox status were chosen for qPCR validation. To this group of validation targets belong mRNAs of the following genes: oxidative stress induced growth inhibitor 1 (OSGIN1), HMOX1, MT2A and GPX2 (Gozzelino et al., 2010; Li et al., 2006; Vašák and Meloni, 2011; Wingler et al., 1999). As the data from the CFE assay indicated cytotoxic effect of 5 nm AuNPs (300 μM, 72 h), we included for qPCR validation two genes encoding regulators of apoptosis: the inhibitor of apoptosis baculoviral IAP repeat containing 2 (BIRC2) and the apoptosis-inducing, DNA binding C1D protein (Dubrez-Daloz et al., 2008; Rothbarth et al., 1999).

We also included gene transcripts of activating transcription factor 1 (ATF1) and genes involved in post-translational protein modifications: histone acetyltransferase 1 (HAT1) and ubiquitin-like modifier SUMO-activating enzyme subunit 2 (UBA2) which is necessary for the sumoylation of proteins (Hay, 2005; Meyer and Habener, 1993; Parthun, 2007). Moreover, the set of mRNAs for validation contains genes encoding DnaJ (Hsp40) homolog, subfamily C, member 21 (DNAJC21), a chaperone which is important for protein translation, folding/unfolding, translocation, and degradation (Qiu et al., 2006); polymerase (DNA directed) kappa (POLK), with a unique DNA-damage bypass and fidelity characteristics (Zhang et al., 2000) and serine/arginine-rich splicing factor 10 (SRSF10) involved in regulation of constitutive and alternative splicing (Shin et al., 2005).

When selecting mRNAs for validation, we also took into consideration the trends in gene expression (up regulation and down regulation) observed in microarray assays, therefore genes which were up (4) and down (8) regulated were included in the qPCR validation test (Table 2). As internal reference genes (RGs), the mRNA transcripts of the c-abl oncogene 1 (ABL1), a non-receptor tyrosine kinase and a mitochondrial ribosomal protein L19 (MRPL19) were used. Under given experimental conditions, these RGs showed to be not affected by exposures of Caco-2 cells to neither size/concentration/exposure time of studied AuNPs (data not shown).

Generally, as shown in Table 2, gene expression levels and trends of regulation (increase/decrease) detected with microarrays *vs* detection and quantification based on qPCR are in agreement with each other. However, expression levels of mRNAs of HAT1 and SRSF10 were lower when detecting them with qPCR, indicating that for these RNA transcripts, the microarray data (300 μM, 72 h) over estimated the levels of their down regulation. On the contrary, for gene BIRC2, HAT1 and MT2A, the qPCR was more sensitive in detecting the alterations of these particular mRNA expression levels (100 μM, 24 and 72 h), where microarrays data was not indicating their decreased RNA transcripts abundances (Table 2).

3.6. Bioinformatics

After validation of transcriptomics data with qPCR, we proceeded with a search for significantly enriched gene classes among differentially expressed genes, as defined by both gene ontology (GO) annotation and KEGG. This was applied to data sets obtained from microarray profiling experiments of Caco-2 cells treated with 5 nm AuNPs (300 μM) and harvested at 24 and 72 h after exposure.

The genes that were down regulated at 24 h time point, show an enrichment of categories related to transcription co-repressor/co-factors activities and transcription factor binding, binding of

Table 3
GO and KEGG enrichment of altered genes (down regulated) by 5 nm AuNPs treatment (300 mM, 24 h). The *p* value refers to how significant an association of a particular term has with the gene list. Where there are more than 10 genes regulated by AuNPs treatment, then only ten most regulated ones are displayed.

Term	Count	*P* value	Genes
GO:0003714 – transcription corepressor activity	6	0.0035	HSBP1, TBL1XR1, SP100, TAF9B, TFEC, C1D
GO:0008134 – transcription factor binding	10	0.0097	HSBP1, RAB18, TBL1XR1, NPM1, UBA2, SP100, TAF9B, TFEC, TADA1, C1D
GO:0003712 – transcription cofactor activity	8	0.0137	HSBP1, TBL1XR1, NPM1, SP100, TAF9B, TFEC, TADA1, C1D
GO:0000287 – magnesium ion binding	9	0.0139	IMPA1, SAR1B, RFK, POLK, HPRT1, MST4, MMGT1, ACVR1C, DUT
GO:0042802 – identical protein binding	11	0.0014	CLDN12 SP100, AK3, NPM1, ATL2, IMPA1, GCA, HPRT1, SNX6, MST4
GO:0032555 – purine ribonucleotide binding	21	0.0276	ATL2, UBE2W, HSPA13, RAB11A, ARL1, RAB18, ARL5B, RP2, MST4, RFK,
GO:0032553 – ribonucleotide binding	21	0.0276	ATL2, UBE2W, HSPA13, RAB11A, ARL1, RAB18, ARL5B, RP2, MST4, RFK,
GO:0017076 – purine nucleotide binding	21	0.0414	ATL2, UBE2W, HSPA13, RAB11A, ARL1, RAB18, ARL5B, RP2, MST4, RFK,
GO:0005525 – GTP binding	7	0.0464	SAR1B, RAB18, ARL5B, AK3, ARL1, ATL2, RAB11A
KEGG:hsa04120:ubiquitin mediated proteolysis	4	0.0537	UBE2N, BIRC2, UBA2, UBE2W

Table 4
GO and KEGG enrichment of altered genes (down regulated) by 5 nm AuNPs treatment (300 μM, 72 h). The *p* value refers to how significant an association of a particular term has with the gene list. Where there are more than 10 genes regulated by AuNPs treatment, then only ten most regulated ones are displayed.

Term	Count	*P* value	Genes
GO:0003723 – RNA binding	37	0.0002	ZCRB1, KIN, STAU2, SNRPB2, DCP2, SRSF3, TRUB1, C1D, EIF1AY, SRP9,
GO:0008270 – zinc ion binding	82	0.0048	RNF219, ZNF124, MOBKL3, PTS, ZFAND6, THAP1, BIRC2, RFK, ZFAND1, PLEKHF2,
GO:0046914 – transition metal ion binding	93	0.0133	RNF219, ZNF124, MOBKL3, PTS, ZFAND6, THAP1, BIRC2, RFK, ZFAND1, PLEKHF2
GO:0031072 – heat shock protein binding	7	0.0141	DNAJB9, DNAJC10, CDK1, DNAJB14, DNAJC19, GNG10, DNAJB6
GO:0004843 – ubiquitin-specific protease activity	4	0.0225	USP33, USP15, USP1, USP16
GO:0016565 – general transcriptional repressor activity	3	0.0224	SP100, HMGB2, CBX3
GO:0019783 – small conjugating protein-specific protease activity	4	0.0253	USP33, USP15, USP1, USP16
GO:0008353 – RNA polymerase II carboxy-terminal domain kinase activity	3	0.0394	MNAT1, CDK1, GTF2H2D
KEGG:hsa00563:glycosylphosphatidylinositol(GPI)-anchor biosynthesis	4	0.0189	PIGA, PIGF, PIGY, PIGK
KEGG:hsa03018:RNA degradation	5	0.0413	C1D, DCP2, CNOT7, LSM5, LSM6
KEGG: hsa00740:riboflavin metabolism	3	0.0510	MTMR6, ACP1, RFK

magnesium and purine (ribo) nucleotide, and ubiquitin mediated proteolysis (Table 3; Suppl. Table I). Examples of genes belonging to these categories include, *e.g.*, HSB1, SP100, TAF9B, MMGT1, POLK, ATL2, RAB18, UBE2N and UBA2. In the group of genes down regulated 72 h after exposure to 5 nm AuNPs, enrichment in categories related to RNA and Zn ion/transition metal ion binding, heat shock protein binding, RNA degradation among others were found (Table 4; Suppl. Table II). These groups of GO/KEGG categories contain proteins encoded by, *e.g.*, genes of STAU2, SRP9, RNF219, BIRC2, DNAJB9, DNAJC21, C1D, DCP2.

As shown in Table 5, the up regulated genes at 72 h after exposure of Caco-2 cells to 5 nm AuNPs (300 μM) turned out to be significantly enriched in GO biological process classes mainly related to ion (Cd and Cu) binding, amino acid/amine transmembrane transporter activity, peptide antigen binding (several MTs and SLC family members) and KEGG pathways, represented by GPX2 and G6PD, involved in the glutathione metabolism. The top highly induced transcripts with 3.55 $\log_2$ fold change (increase in the mRNA levels of about 12 times) belong to genes encoding metallothioneins (MTs).

In humans, there are at least 18 genes encoding four distinct isoforms of MTs proteins: MT1, MT2, MT3 and MT4 (Laukens et al., 2009). The sequence homology grouping of MTs mRNAs is shown in Suppl. Fig. 3A. For the construction of phylogenetic trees, all members of the human MT gene family were plotted and analyzed against the mRNA of MT2A as a reference sequence. The MTs which mRNAs were induced in Caco-2 cells treated with 5 nm AuNPs (300 μM, 72 h) are in red, while the MTs which expression was not altered by exposure are in black. The exposure of Caco-2 cells to 5 nm AuNPs (300 μM, 72 h) resulted in up regulation of seven MTs mRNAs belonging to MT1 and MT2 groups only. Actually, there are 6 mRNAs of MTs (MT2A, MT1l, MT1E, MT1B, MT1X and MT1H) among 10 top up regulated genes (Suppl. Fig. 3B), with the most highly up regulated gene being the MT2A. Noteworthy, the increased mRNA level of MT2A gene detected in the microarray assay was confirmed with qPCR (Table 2).

When we analysed functions of genes which were among the highly down regulated (Suppl. Fig. 3C), the gene encoding selenoprotein T (SELT) was noticed once more. The SELT attracted our attention because another selenoprotein, namely GPX2 was highly up regulated (Tables 2 and 5) under the same exposure conditions (5 nm AuNP, 300 μM, 72 h).

The data analysis for information on mRNA co-expression and protein-protein interaction of highly up-regulated genes (MT2A, GPX2 and G6PD) and their connections with oxidative stress pathway [Hs_Oxidative_Stress_WP408_38774] revealed that MT2A is connected with 1 gene, while G6PD is connected with 5 genes belong to this biological network (Suppl. Fig. 4A). Notably, the MT1X gene, connected with MT2A, is also up regulated by 5 nm AuNPs (300 μM, 72 h). When looking at interactomes of most significantly up regulated and down regulated genes, the following was found: (i) in the set of genes which were up regulated, grouping of MTs genes with their mRNA and protein co-regulation was observed (Suppl. Fig. 4B); (ii) the density of mRNA/protein co-expression networks of up regulated genes was not as dense as for genes which were significantly down regulated (Suppl. Fig. 4C) and showed strong connections between each other.

The observation of a high number of down regulated RNA transcripts in Caco-2 cells exposed to 5 nm AuNPs, in particular at 72 h time point (300 μM), raised a question: at which level the repression of genes might have occurred? With the microarrays data in hand and with the freely available DIANA mirExTra tool for predicting potential microRNAs (miRNAs) binding targets sequences in differentially expressed mRNAs, we decided to run an *in silico* experiment. In this way, we were able to probe 25 most significantly down regulated genes, in parallel with 50 not affected by AuNPs (control genes), for analyzing *ad hoc* potential epigenetic regulators of gene expression, at miRNA-mRNA interface levels (Flynt and Lai, 2008). The results of the prediction test are presented in Suppl. Table III and in Fig. 5.

We found that, the following miRNAs: miR 340, miR 181a, miR 410 and miR 520 d 5p (Fig. 5A), are being frequently identified by

Table 5
The *p* value refers to how significant an association of a particular term has with the gene list.

Term	Count	*P* value	Genes
GO:0046870 – cadmium ion binding	4	0.0000026	MT1L, MT1A, MT1B, MT1F
GO:0005507 – copper ion binding	4	0.0009	MT1L, MT1A, MT1B, MT1F
GO:0015171 – amino acid transmembrane transporter activity	3	0.0117	SLC6A6, SLC7A5, SLC43A2
GO:0005275 – amine transmembrane transporter activity	3	0.0182	SLC6A6, SLC7A5, SLC43A2
GO:0042605 – peptide antigen binding	2	0.0341	SLC7A5, CLEC4M
KEGG:Hsa00480:glutathione metabolism	2	0.0999	GPX2, G6PD

Fig. 5. Predicted miRs with the corresponding target genes that were decreased upon exposure of Caco-2 cells to 5 nm AuNPs (300 μM, 72 h). Group of miRs having 5–9 predicted target mRNAs (A). Set of genes with the highest number of predicted miRs binding sites in their mRNAs sequences (B). In gray are indicated mRNAs with no miRs binding site prediction. Asterics (*) denotes the most down regulated genes. Both word clouds were generated using the data presented in Suppl. Table 3.

the DIANA mirExTra algorithm and might represent potential mediators of down regulation of several mRNAs in the analyzed data set (Fig. 5B). Interestingly, the most down regulated genes (ZCCHC10, MAD2L1, C13orf27, CNPK, COMMD8) were not among the best targets for miRNAs mediated post-transcriptional gene regulation in the given experimental data set prediction context (Suppl. Table III, Fig. 5B). On the contrary, gene encoding selenoprotein SELT has 12 predicted binding sites for miRNAs, in the same number range for predicted miRNA binding sites (10–17), as the other down regulated genes have (PLDN, TMEM38B, ARL6IP6, C14orf129 and GOLT1B). The gene that has the highest number of predicted miRNAs binding sites (27), encodes mesoderm induction early response 1, family member 3 protein (MIER3).

4. Discussion

Several factors are involved in determining cytotoxicity of engineered nanomaterials (ENMs). Our work focused mainly on comparing cytotoxic potentials, in the context of inhibitory effect on colony forming efficiency (CFE) with changes in gene expression patterns (transcriptomics) induced in Caco-2 cells exposed to 5 nm and 30 nm citrate-stabilized AuNPs. Chemico-physical characterization tests of AuNPs used in this study confirmed that AuNPs were of expected size/shape and behaved in the experimental media as previously reported by Coradeghini et al. (2013).

In this work we selected undifferentiated Caco-2 cells an *in vitro* model of the intestinal route of exposure to nanoparticles. When Caco-2 cells are cultured over confluence for 21 days, these cells undergo spontaneous cell cycle arrest and differentiation. In his process, the enterocyte-like monolayer is formed serving as a model of the intestinal barrier (Sambuy et al., 2005; Natoli et al., 2012). Due to the intrinsic heterogeneity of the original parental cell line and culture-related conditions upon differentiation the expression of morphological and functional characteristics of mature enterocytes varies greatly between experiments and laboratories. Taking this into consideration, we have chosen to use in our work undifferentiated Caco-2 cultures to study their biological responses to AuNPs exposure. In this way we looked at populations of heterogenic pool of Caco-2 cells prior to differentiation, therefore having wider plasticity in the cellular physiology, sensing and adaptation/response to stress, as compared to mature and polarized enterocytes (Tadiali et al., 2002). Keeping this in mind, when running both the cytotoxicity and RNA transcript profiling experiments, we explored Caco-2 cells (in undifferentiated stage) as potentially more suitable model for detecting alterations in gene expression patterns upon exposure to NPs. We have to stress, that in that particular case, undifferentiated Caco-2 cells might have shown culture growth condition specific routes and efficiency in uptake of NPs. This in turn may contributed in part to alternative cellular responses to stress and gene expression patterns, as compared with possibly different responses of classical model of mature enterocyte-like Caco-2 monolayer cells (Tremblay et al., 2006; Natoli et al., 2011).

When exposed to AuNPs, Caco-2 cells efficiently uptake AuNPs at both incubation times tested (24 and 72 h). However, we did not detect further increase in cellular uptake at later time point (72 h), maybe due to reaching of a steady-state of the uptake. These findings are in line with data reported earlier, supporting the notion that extending the incubation times above 24 h might not be useful for enhancing cellular uptake of nanoparticles, as observed in primary HUVECs, C17.2 neural progenitor cells and rat PC12 cells (Soenen et al., 2012), but in contrast with results obtained with mouse Balb/3T3 cells (Coradeghini et al., 2013). In the later case, time dependent increase in uptake of AuNPs, even after 24 h exposure time, was observed. We have also observed that if we express the uptake in number of NPs/cell or % of AuNPs versus total exposure, at the same external dose of exposure, the 5 nm AuNPs cell internalisation is higher than 30 nm AuNPs. This result is probably due to the fact that cells are exposed to a number of small NPs that is approximately 100 times higher than bigger NPs. In addition, as previously observed for Balb/3T3 cells (Coradeghini et al., 2013) by TEM analysis, both 5 and 30 nm NPs are internalised by endocytic patway.

When testing cytotoxic effects of AuNPs at the cellular level, we observed inhibition of Caco-2 cell growth and decrease in colony forming efficiency, induced by smaller AuNPs (5 nm). We must admit that this cytotoxic effect was observed only at relatively high levels of exposure (200 μM and 300 μM), with the most evident inhibitory effect detected at concentration 300 μM at 72 h. At the molecular level, when measuring biomarkers related to AuNPs exposures by changes in RNA expression levels, broad range of responses which potentially mediate inhibition of cellular growth and other functions of Caco-2 cells in response to nano gold, were identified. These cellular processes affected by exposure to 5 nm AuNPs include, for the early time point examined (24 h), down regulation of genes involved in regulation of transcription (transcriptional factors), biogenesis of RNA and GTP binding among others. At the later time point studied (72 h), more dramatic changes in differentially expressed gene expression patterns evoked by 5 nm AuNPs were detected. Beside 708 down regulated genes, an increase in abundance of 103 RNA transcripts was also observed. Thus, our gene expression profiling experiments demonstrated that RNA/zinc ion/transition metal ion binding, heat shock protein binding, RNA degradation and splicing (decreased); cadmium/copper ion binding, amino acid/amine transmembrane transporter activity and glutathione metabolism (increased), were among the cellular response processes correlated with exposure of Caco-2 cells and were associated with cytotoxicity induced by smaller AuNPs (5 nm, 300 μM).

Interestingly, although the larger (30 nm) AuNPs had rather limited effect on Caco-2 cell mRNAs expression, these AuNPs were still able to induce expression of couple of genes already at 100 μM exposure level at 24 h time point (CDH16, CPA2, TSC22D3 and CRIPAK). Noteworthy, the CDH16 protein was shown to be exclusively expressed in the kidney (Thomson et al., 1995); however its mRNA transcript induction was evident when the Caco-2 cells, originating from the colon, were exposed to 30 nm AuNPs.

As mentioned earlier, treatment of cells with 5 nm AuNPs had very pronounced effect on increase in mRNAs levels of metallothioneins (MTs) genes belonging to the MT1 and MT2 isoforms only. Exposure to nano gold had no effect on the MT3 or MT4 mRNAs expression in Caco-2 cells (gastrointestinal origin) due to the fact that MT3 is usually expressed in neurons (Masters et al., 1994), while MT4 is exclusively found in stratified squamous epithelium (Quaife et al., 1994).

Differential expression of selenoproteins (GPX2↑ while SELT, SEPP1, SELK and 15 kDa selenoprotein↓), might be related to changes in levels of selenium. Selenoproteins belong to a group of proteins which play important role in, *e.g.*, oxidative stress signaling and protection, redox homeostasis, thyroid hormone metabolism, protection of some forms of cancer among others (Papp et al., 2010). It has been shown that the mRNA stability of selenoproteins differs depending on the availability of selenium within the cell (Schomburg and Schweizer, 2009). Therefore, we have hypothesized that Caco-2 cells might have responded to high concentration of AuNPs as if they have faced selenium "deficiency". It is also possible that high concentration of gold within the cell or/and extra cellular milieu had an effect on selenium homeostasis or/and its availability for uptake by Caco-2 cells.

Lowered cellular selenium content can evoke Nrf2 and Wnt stress response signaling *via* disturbed redox state as demonstrated by Brigelius-Flohé and Kipp (2013). The changes we found in expression of genes belonging to Nrf2 mediated signaling cascades (metallothioneins, HMOX, OSGIN1, G6PD, GPX2 and other selenoproteins) are indeed well described targets of regulation by transcriptional factor Nrf2 (Kensler et al., 2007; Miles et al., 2000). Therefore, changes in expression of genes being under Nrf2 control and induced by small AuNPs (5 nm) might be the result of different triggers: metal exposure, oxidative stress, disturbed redox and selenium status, and/or combination of them. Noteworthy, it was recently observed that Nrf2 is activated in Caco-2 cells upon exposure to high concentrations of silver NPs (Aueviriyavit et al., 2014) supporting our reasoning that induction of mRNA levels of the genes mentioned above, involves Nrf2 mediated signaling events, at least to some extent.

The results presented here clearly indicate that the cancer cells used in this study were able to recognize the AuNPs not only as metal entities but also as potential "danger" signals and stress inducers. Although Caco-2 cells showed the capacity to activate Nrf2-mediated defense networks (Kensler et al., 2007), these responses were not sufficient in preventing toxic effect of 5 nm AuNPs that were observed in CFE assay. Consequently, stress resulting from cytotoxic level of smaller AuNPs had an effect on down regulation of genes important for RNA biogenesis (transcription, splicing) and post-translational modifications (ubiquitination, sumoylation) of proteins that are vital for protein stability, activity and turn-over (proteolysis), especially when the misfolding of proteins occurs, for example during oxidative stress. Therefore, Caco-2 cells exhibited slower growth and lower efficiency in forming colonies.

It is well known that gene expression can be regulated at chromatin level (histone code) and RNA level (transcription, splicing, post-transcriptional RNA modifications, RNA stability/turn over of RNA transcripts, cellular localization of RNA molecules, their translation *etc.*). These processes quite often involve and are regulated by non-coding RNAs (ncRNAs), including small (20–22 nt long) non-coding microRNAs (Venkatesh et al., 2013; Ullah et al., 2014). For that reason, we tested *in silico* the microarrays expression data for the presence of miRNAs binding sites across highly down regulated mRNAs (300 μM, 72 h, 5 nm AuNP). Indeed, prediction analysis pointed out that some miRNAs (miR 340, miR 181a, miR 410, miR 520 d5p) could play to some extend a role in down regulating many of tested mRNA targets.

The explanation of the very weak response of Caco-2 cells at transcriptome level, upon exposure to larger AuNPs (30 nm), remains still unclear. When interpreting our results the following explanation(s) can be suggested. As already reported in literature, the cellular uptake of engineered nanoparticles depends on the size of nanoparticles (Wang et al., 2010; Labens et al., 2013; Li and Schneider, 2014). In our experimental settings, the number of AuNPs taken up by the cells is much higher in the case of smaller NPs (5 nm), and this by itself might represent more biologically significant "stimulus". Thereafter, combination of the frequency of cellular membrane association/engulfment, uptake and exocytosis of 5 nm AuNPs, may trigger much stronger effect on signaling events, as compared to 30 nm AuNPs that are present in lower number but at the same molar Au concentration (Bahrami et al., 2014; Oh and Park, 2014). Moreover, it is also possible that smaller AuNPs (5 nm), with higher surface area to volume ratio, resulting in higher reactivity toward biological molecules (Nel et al., 2009), are more "disruptive" to the homeostasis of exposed cells as compared to larger AuNPs (30 nm). The different expression profiles observed in Caco-2 cells exposed to the two different sizes of nano gold particles, gave an additional support to previously published findings demonstrating that isotropic AuNPs larger than 5 nm seem to be biologically inert (Li et al., 2014).

We must stress however, that although the larger AuNPs showed very limited activity at transcriptional level, the picture of cellular responses might be different when looking at different exposure time (*e.g.*, earlier sampling time), end-points/markers (protein expression, post-translational modifications, cellular metabolism, intracellular trafficking/secretion of bio-molecules, *etc.*). Also, the fact that Caco-2 cells were exposed to much higher number of small AuNPs as compared to larger AuNPs, points out that some cytotoxic effects might be observed even for 30 nm AuNPs, if given to cells in adequately higher numbers.

Interestingly, Caco-2 cells actually responded to 30 nm AuNPs already at 24 h by up regulating four gene transcripts after being exposed to this AuNPs (100 μM). Notably, under the same exposure conditions, presence of 5 nm AuNPs in the cell culture medium and/or as adsorbed/internalized AuNPs by cells, did not affect gene expression patterns in Caco-2 cells. One possible explanation is that the mass transfer of larger AuNPs (30 nm) to the cellular surface and interaction with cellular membrane, as a result of more rapid gravitational settling/sedimentation (Wittmaack, 2011; Li and Schneider, 2014) which is higher as compared to smaller AuNPs, triggering diverse signaling events, at different time points and with possible different effects on gene expression as compared to these evoked by exposure to 5 nm AuNPs.

The observed cytotoxic properties of smaller AuNPs might be of practical use for enhancement of already existing AuNPs based thermal therapies, as well as in other cancer treatment regimes (Schütz et al., 2013). Nevertheless, we should not ignore the fact that changes in gene expression induced by 5 nm AuNPs exposure might lead to potentially hazardous effect for healthy cells and/or tissues that still need to be estimated and characterized despite the absence of acute toxicity effects. This is of great concern, especially for individuals who are undergoing long-term AuNPs-based treatment.

5. Conclusions

A combination of standard cytotoxicity methods, such as CFE and Trypan blue exclusion assays, with gene expression profiling (transcriptomics) allowed us to identify cellular signaling and stress response pathways that might be associated with the cytotoxicity observed upon exposure of Caco-2 cells to citrate-stabilized AuNPs (5 nm). However, it is critical to point out that changes in gene expression at mRNA level do not necessarily correlate with observed trends (up/down regulation) in the amount of corresponding protein (Walker and Hughes, 2008). Therefore, validation(s) of alterations in mRNA expression, observed in Caco-2 cells as response to AuNPs exposures, requires further work to estimate the changes in the corresponding expression of encoded protein(s), their activity, proper localization and/or secretion. The very same approach also applies for testing whatever the predicted involvement of miRNAs and/or other ncRNAs takes place and might contribute to cellular responses evoked by treatment of Caco-2 cells with AuNPs.

Nevertheless, data presented here provide a starting point in exploration of possible mechanisms related to cytotoxicity observed in cells exposed to AuNPs and can be applied for designing more efficient and safe nano gold nanomedicines.

Funding

This work was supported by the European Commission DG Joint Research Centre (Work Program Action 15024 and 15014) for Nanobiosciences (NBS) Unit and Chemical Assessment and Testing (CAT) Unit respectively, of the Institute for Health and Consumer Protection (IHCP) at European Commission Joint Research Centre (JRC), Ispra, Italy.

Transparency document

The Transparency document associated with this article can be found in the online version.

Conflict of interest

The authors declare that there are no conflicts of interest.

Acknowledgements

M. Fabbri is enrolled in Ph.D. program in Biotechnology, School of Biological Sciences, University of Insubria, Varese, Italy. We are thankful to Dr. Fabio Franchini for performing the ICP-MS analysis of AuNPs cellular uptake and Dr. Rita La Spina for synthesis of AuNPs.

Appendix A. Supplementary data

Supplementary data associated with this article can be found, in the online version, at http://dx.doi.org/10.1016/j.toxlet.2014.12.008.

References

Alexeyenko, A., Schmitt, T., Tjärnberg, A., Guala, D., Frings, O., Sonnhammer, E.L., 2011. Comparative interactomics with Funcoup 2.0. Nucleic Acids Res. 40, D821–D828. doi:http://dx.doi.org/10.1093/nar/gkr1062.

Alexiou, P., Maragkakis, M., Papadopoulos, G.L., Simmosis, V.A., Zhang, L., Hatzigeorgiou, A.G., 2010. The DIANA-mirExTra web server: from gene expression data to microRNA function. PLoS One 5, e9171. doi:http://dx.doi.org/10.1371/journal.pone.0009171.

Auevirivavit, S., Phummiratch, D., Maniratanachote, R., 2014. Mechanistic study on the biological effects of silver and gold nanoparticles in Caco-2 cells induction of the Nrf2/HO-1 pathway by high concentrations of silver nanoparticles. Toxicol. Lett. 224, 73–83. doi:http://dx.doi.org/10.1016/j.toxlet.2013.09.020.

Ayroldi, E., Riccardi, C., 2009. Glucocorticoid-induced leucine zipper (GILZ): a new important mediator of glucocorticoid action. FASEB J. 23, 3649–3658. doi:http://dx.doi.org/10.1096/fj.09-134684.

Bahrami, A.H., Raatz, M., Agudo-Canalejo, J., Michel, R., Curtis, E.M., Hall, C.K., Gradzielski, M., Lipowsky, R., Weikl, T.R., 2014. Wrapping of nanoparticles by membranes. Adv. Colloid. Interface Sci. 208, 214–224. doi:http://dx.doi.org/10.1016/j.cis.2014.02.012.

Bhattacharya, R., Mukherjee, P., 2008. Biological properties of naked metal nanoparticles. Adv. Drug Deliv. Rev. 60, 1289–1306. doi:http://dx.doi.org/10.1016/j.addr.2008.03.013.

Bolstad, B.M., Irizarry, R.A., Astrand, M., Speed, T.P., 2003. A comparison of normalization methods for high density oligonucleotide array data based on variance and bias. Bioinformatics 19, 185–193. doi:http://dx.doi.org/10.1093/bioinformatics/19.2.185.

Brigelius-Flohé, R., Kipp, A.P., 2013. Selenium in the redox regulation of the Nrf2 and the Wnt pathway. Methods Enzymol. 527, 65–86. doi:http://dx.doi.org/10.1016/B978-0-12-405882-8.00004-0.

Chovatiya, R., Medzhitov, R., 2014. Stress, inflammation, and defense of homeostasis. Mol. Cell. 54, 281–288. doi:http://dx.doi.org/10.1016/j.molcel.2014.03.030.

Chuang, S.M., Lee, Y.H., Liang, R.Y., Roam, G.D., Zeng, Z.M., Tu, H.F., Wang, S.K., Chueh, P.J., 2013. Extensive evaluations of the cytotoxic effects of gold nanoparticles. Biochim. Biophys. Acta 496, 4960–4973. doi:http://dx.doi.org/10.1016/j.bbagen.2013.06.025.

Connor, E.E., Mwamuka, J., Gole, A., Murphy, C.J., Wyatt, M.D., 2005. Gold nanoparticles are taken up by human cells but do not cause acute cytotoxicity. Small 1, 325–327. doi:http://dx.doi.org/10.1002/smll.200400093.

Coradeghini, R., Gioria, S., García, C.P., Nativo, P., Franchini, F., Gilliland, D., Ponti, J., Rossi, F., 2013. Size-dependent toxicity and cell interaction mechanisms of gold nanoparticles on mouse fibroblasts. Toxicol. Lett. 217, 205–216. doi:http://dx.doi.org/10.1016/j.toxlet.2012.11.022.

Dubchak, I., Munoz, M., Poliakov, A., Salomonis, N., Minovitsky, S., Bodmer, R., Zambon, A.C., 2013. Whole-Genome rVISTA: a tool to determine enrichment of transcription factor binding sites in gene promoters from transcriptomic data. Bioinformatics 129, 2059–2061. doi:http://dx.doi.org/10.1093/bioinformatics/btt318.

Dubrez-Daloz, L., Dupoux, A., Cartier, J., 2008. IAPs: more than just inhibitors of apoptosis proteins. Cell Cycle 7, 1036–1046. doi:http://dx.doi.org/10.4161/cc.7.8.5783.

Dykman, L., Khlebtsov, N., 2012. Gold nanoparticles in biomedical applications: recent advances and perspectives. Chem. Soc. Rev. 41, 2256–2282. doi:http://dx.doi.org/10.1039/c1cs15166e.

Esther, R.J., Bhattacharya, R., Ruan, M., Bolander, M.E., Mukhopadhyay, M.E., Sarkar, D., Mukherjee, G., 2005. Gold nanoparticles do not affect the global transcriptional program of human umbilical vein endothelial cells: a DNA microarray analysis. J. Biomed. Nanotechnol. 3, 328–335.

Evers, B.M., 2006. Neurotensin and growth of normal and neoplastic tissues. Peptides 27, 2424–2433. doi:http://dx.doi.org/10.1016/j.peptides.2006.01.028.

Flynt, A.S., Lai, E.C., 2008. Biological principles of microRNA-mediated regulation: shared themes amid diversity. Nat. Rev. Genet. 9, 831–842. doi:http://dx.doi.org/10.1038/nrg2455.

Fukuda, S., Yamasaki, Y., Iwaki, T., Kawasaki, H., Akieda, S., Fukuchi, N., Tahira, T., Hayashi, K., 2002. Characterization of the biological functions of a transcription factor, c-myc intron binding protein 1 (MIBP1). J. Biochem. 131, 349–357.

Fulda, S., Gorman, A.M., Hori, O., Samali, A., 2010. Cellular stress responses: cell survival and cell death. Int. J. Cell. Biol. 2010, 214074. doi:http://dx.doi.org/10.1155/2010/214074.

Gentleman, R.C., Carey, V.J., Bates, D.M., Bolstad, B., Dettling, M., Dudoit, S., Ellis, B., Gautier, L., Ge, Y., Gentry, J., et al., 2004. Bioconductor: open software development for computational biology and bioinformatics. Genome Biol. 5, R80. doi:http://dx.doi.org/10.1186/gb-2004-5-10r80.

Gioria, S., Chassaigne, H., Carpi, D., Parracino, A., Meschini, S., Barboro, P., Rossi, F., 2014. A proteomic approach to investigate AuNPs effects in Balb/3T3 cells. Toxicol. Lett. 228, 111–126. doi:http://dx.doi.org/10.1016/j.toxlet.2014.04.016.

Gozzelino, R., Jeney, V., Soares, M.P., 2010. Mechanisms of cell protection by heme oxygenase-1. Annu. Rev. Pharmacol. Toxicol. 50, 323–354. doi:http://dx.doi.org/10.1146/annurev.pharmtox.010909.105600.

Hainfeld, J.F., Slatkin, D.N., Focella, T.M., Smilowitz, H.M., 2006. Gold nanoparticles: a new X-ray contrast agent. Br. J. Radiol. 79, 248–253. doi:http://dx.doi.org/10.1259/bjr/13169882.

Haiss, W., Thanh, N.T.K., Aveyard, J., Fernig, D.G., 2007. Determination of size and concentration of gold nanoparticles from UV–vis spectra. Anal. Chem. 79, 4215–4221. doi:http://dx.doi.org/10.1021/ac0702084.

Hamadeh, H.K., Amin, R.P., Paules, R.S., Afshari, C.A., 2002. An overview of toxicogenomics. Curr. Issues Mol. Biol. 4, 45–56.

Hay, R.T., 2005. SUMO: a history of modification. Mol. Cell. 18, 1–12. doi:http://dx.doi.org/10.1016/j.molcel.2005.03.012.

Kensler, T.W., Wakabayashi, N., Biswal, S., 2007. Cell survival responses to environmental stresses via the Keap1-Nrf2-ARE pathway. Annu. Rev. Pharmacol. Toxicol. 47, 89–116. doi:http://dx.doi.org/10.1146/annurev.pharmtox.46.120604.141046.

Kunzmann, A., Andersson, B., Thurnherr, T., Krug, H., Scheynius, A., Fadeel, B., 2011. Toxicology of engineered nanomaterials: focus on biocompatibility,

biodistribution and biodegradation. Biochim. Biophys. Acta 1810, 361–373. doi:http://dx.doi.org/10.1016/j.bbagen.2010.04.007.
Labens, R., Lascelles, B.D., Charlton, A.N., Ferrero, N.R., Van Wettere, A.J., Xia, X.R., Blikslager, A.T., 2013. Ex vivo effect of gold nanoparticles on porcine synovial membrane. Tissue Barriers 1, e24314. doi:http://dx.doi.org/10.4161/tisb.24314.
Laukens, D., Waeytens, A., De Bleser, P., Cuvelier, C., De Vos, M., 2009. Human metallothionein expression under normal and pathological conditions: mechanisms of gene regulation based on in silico promoter analysis. Crit. Rev. Eukaryot. Gene Expression 19, 301–317. doi:http://dx.doi.org/10.1615/CritRevEukarGeneExpr.v19. i4.40.
Li, K., Schneider, M., 2014. Quantitative evaluation and visualization of size effect on cellular uptake of gold nanoparticles by multiphoton imaging-UV/vis spectroscopic analysis. J. Biomed. Opt. 19, 101505. doi:http://dx.doi.org/10.1117/1. JBO.19.10.101505.
Li, R., Chen, W., Yanes, R., Lee, S., Berliner, J.A., 2006. OKL38 is an oxidative stress response gene stimulated by oxidized phospholipids. J. Lipid Res. 48, 709–715. doi:http://dx.doi.org/10.1194/jlr.M600501-JLR200.
Li, J.J., Lo, S.L., Ng, C.T., Gurung, R.L., Hartono, D., Hande, M.P., Ong, C.N., Bay, B.H., Yung, L.Y., 2011. Genomic instability of gold nanoparticle treated human lung fibroblast cells. Biomaterials 32, 5515–5523. doi:http://dx.doi.org/10.1016/j.biomaterials.2011.04.023.
Li, N., Zhao, P., Astruc, D., 2014. Anisotropic gold nanoparticles: synthesis, properties, applications, and toxicity. Angew. Chem. Int. Ed. Engl. 53, 1756–1789. doi:http://dx.doi.org/10.1002/anie.201300441.
Livak, K.J., Schmittgen, T.D., 2001. Analysis of relative gene expression data using real-time quantitative PCR and the 2(-Delta Delta C(T)) method. Methods 25, 402–408. doi:http://dx.doi.org/10.1006/meth.2001.1262.
Masters, B.A., Quaife, C.J., Erickson, J.C., Kelly, E.J., Froelick, G.J., Zambrowicz, B.P., Brinster, R.L., Palmiter, R.D., 1994. Metallothionein III is expressed in neurons that sequester zinc in synaptic vesicles. J. Neurosci. 14, 5844–5857.
Maynard, R.L., 2012. Nano-technology and nano-toxicology. Emerg. Health Threats J. 5, 17508. doi:http://dx.doi.org/10.3402/ehtj.v5i0.17508.
Meyer, T.E., Habener, J.F., 1993. Cyclic adenosine 3′,5′-monophosphate response element binding protein (CREB) and related transcription-activating deoxyribonucleic acid-binding proteins. Endocr. Rev. 14, 269–290. doi:http://dx.doi.org/10.1210/edrv-14-3-269.
Miles, A.T., Hawksworth, G.M., Beattie, J.H., Rodilla, V., 2000. Induction regulation, degradation, and biological significance of mammalian metallothioneins. Crit. Rev. Biochem. Mol. Biol. 35, 35–70.
Mironava, T., Hadjiargyrou, M., Simon, M., Rafailovich, M.H., 2014. Gold nanoparticles cellular toxicity and recovery: adipose derived stromal cells. Nanotoxicology 8, 189–201. doi:http://dx.doi.org/10.3109/17435390.2013.769128.
Natoli, M., Leoni, B.D., D'Agnano, I., D'Onofrio, M., Brandi, R., Arisi, I., Zucco, F., Felsani, A., 2011. Cell growing density affects the structural and functional properties of Caco-2 differentiated monolayer. J. Cell Physiol. 226 (6), 1531–1543. doi:http://dx.doi.org/10.1002/jcp.22487.
Natoli, M., Leoni, B.D., D'Agnano, I., Zucco, F., Felsani, A., 2012. Good Caco-2 cell culture practices. Toxicol. In Vitro 26 (8), 1243–1246. doi:http://dx.doi.org/10.1016/j.tiv.2012.03.009.
Nel, A.E., Mädler, L., Velegol, D., Xia, T., Hoek, E.M., Somasundaran, P., Klaessig, F., Castranova, V., Thompson, M., 2009. Understanding biophysicochemical interactions at the nano-bio interface. Nat. Mater. 8, 543–557. doi:http://dx.doi.org/10.1038/nmat2442.
Oh, N., Park, J.-H., 2014. Endocytosis and exocytosis of nanoparticles in mammalian cells. Int. J. Nanomed. 9 (Suppl. 1), 51–63. doi:http://dx.doi.org/10.2147/IJN.S26592.
Oku, S., Takahashi, N., Fukata, Y., Fukata, M., 2013. In silico screening for palmitoyl substrates reveals a role for DHHC1/3/10 (zDHHC1/3/11)-mediated neurochondrin palmitoylation in its targeting to Rab5-positive endosomes. J. Biol. Chem. 288, 19816–19829. doi:http://dx.doi.org/10.1074/jbc.M112.431676.
Papp, L.V., Holmgren, A., Khanna, K.K., 2010. Selenium and selenoproteins in health and disease. Antioxid. Redox Signal. 12, 793–795. doi:http://dx.doi.org/10.1089/ars.2009.2973.
Parthun, M.R., 2007. Hat1: the emerging cellular roles of a type B histone acetyltransferase. Oncogene 26, 5319–5328. doi:http://dx.doi.org/10.1038/sj.onc.1210602.
Pernodet, N., Fang, X., Sun, Y., Bakhtina, A., Ramakrishnan, A., Sokolov, J., Ulman, A., Rafailovich, M., 2006. Adverse effects of citrate/gold nanoparticles on human dermal fibroblasts. Small 2, 766–773. doi:http://dx.doi.org/10.1002/smll.200500492.
Ponti, J., Colognato, R., Rauscher, H., Gioria, S., Broggi, F., Franchini, F., Pascual, C., Giudetti, G., Rossi, F., 2010. Colony forming efficiency and microscopy analysis of multi-wall carbon nanotubes cell interaction. Toxicol. Lett. 197, 29–37. doi:http://dx.doi.org/10.1016/j.toxlet.2010.04.018.
Qiu, X.B., Shao, Y.M., Miao, S., Wang, L., 2006. The diversity of the DnaJ/Hsp40 family, the crucial partners for Hsp70 chaperones. Cell. Mol. Life Sci. 63, 2560–2570. doi:http://dx.doi.org/10.1007/s00018-006-6192-6.
Qu, Y., Huang, Y., Lü, X., 2013. Proteomic analysis of molecular biocompatibility of gold nanoparticles to human dermal fibroblasts-fetal. J. Biomed. Nanotechnol. 9, 40–52. doi:http://dx.doi.org/10.1166/jbn.2013.1428.
Quaife, C.J., Findley, S.D., Erickson, J.C., Froelick, G.J., Kelly, E.J., Zambrowicz, B.P., Palmiter, R.D., 1994. Induction of a new metallothionein isoform (MT-IV) occurs during differentiation of stratified squamous epithelia. Biochemistry 33, 7250–7259. doi:http://dx.doi.org/10.1021/bi00189a029.
Rothbarth, K., Spiess, E., Juodka, B., Yavuzer, U., Nehls, P., Stammer, H., Werner, D., 1999. Induction of apoptosis by overexpression of the DNA-binding and DNA-PK-activating protein C1D. J. Cell Sci. 112, 2223–2232.
Sambuy, Y., De Angelis, I., Ranaldi, G., Scarino, M.L., Stammati, A., Zucco, F., 2005. The Caco-2 cell line as a model of the intestinal barrier: influence of cell and culture-related factors on Caco-2 cell functional characteristics? Altern. Lab. Anim. 33 (6), 603–618.
Schütz, C.A., Juillerat-Jeanneret, L., Mueller, H., Lynch, I., Riediker, M., 2013. Therapeutic nanoparticles in clinics and under clinical evaluation. Nanomedicine 8, 449–467. doi:http://dx.doi.org/10.2217/nnm.13.8.
Schomburg, L., Schweizer, U., 2009. Hierarchical regulation of selenoprotein expression and sex-specific effects of selenium. Biochim. Biophys. Acta 1790, 1453–1462. doi:http://dx.doi.org/10.1016/j.bbagen.2009.03.015.
Shelton, P., Jaiswal, A.K., 2013. The transcription factor NF-E2-related factor 2 (Nrf2): a protooncogene? FASEB J. 27, 414–423. doi:http://dx.doi.org/10.1096/fj.12-217257.
Shin, C., Kleiman, F.E., Manley, J.L., 2005. Multiple properties of the splicing repressor SRp38 distinguish it from typical SR proteins. Mol. Cell. Biol. 25, 8334–8343. doi:http://dx.doi.org/10.1128/MCB.25.18.8334-8343.2005.
Smyth, G.K., 2004. Linear models and empirical bayes methods for assessing differential expression in microarray experiments. Stat. Appl. Genet. Mol. Biol. 3, 1–25. doi:http://dx.doi.org/10.2202/1544-6115.1027 (Article 3).
Soenen, S.J., Manshian, B., Montenegro, J.M., Amin, F., Meermann, B., Thiron, T., Cornelissen, M., Vanhaecke, F., Doak, S., Parak, W.J., et al., 2012. Cytotoxic effects of gold nanoparticles: a multiparametric study. ACS Nano 6, 5767–5783. doi:http://dx.doi.org/10.1021/nn301714n.
Staggers, N., McCasky, T., Brazelton, N., Kennedy, R., 2008. Nanotechnology: the coming revolution and its implications for consumers, clinicians, and informatics. Nurs. Outlook 56, 268–274. doi:http://dx.doi.org/10.1016/j.outlook.2008.06.004.
Tadiali, M., Seidelin, J.B., Olsen, J., Troelsen, J.T., 2002. Transcriptome changes during intestinal cell differentiation. Biochim. Biophys. Acta 1589 (2), 160–167.
Talukder, A.H., Meng, Q., Kumar, R., 2006. CRIPak a novel endogenous Pak1 inhibitor. Oncogene 25, 1311–1319. doi:http://dx.doi.org/10.1038/sj.onc.1209172.
Thomson, R.B., Igarashi, P., Biemesderfer, D., Kim, R., Abu-Alfa, A., Soleimani, M., Aronson, P.S., 1995. Isolation and cDNA cloning of Ksp-cadherin, a novel kidney-specific member of the cadherin multigene family. J. Biol. Chem. 270, 17594–17601. doi:http://dx.doi.org/10.1074/jbc.270.29.17594.
Tremblay, E., Auclair, J., Delvin, E., Levy, E., Ménard, D., Pshezhetsky, A.V., Rivard, N., Seidman, E.G., Sinnett, D., Vachon, P.H., Beaulieu, J.F., 2006. Gene expression profiles of normal proliferating and differentiating human intestinal epithelial cells: a comparison with the Caco-2 cell model? J. Cell Biochem. 99 (4), 1175–1186.
Turkevich, J., Stevenson, P.C., Hillier, J., 1951. A study of nucleation and growth process in the synthesis of colloidal gold. Discuss. Faraday Soc. 11, 55–75.
Ullah, S., John, P., Bhatti, A., 2014. MicroRNAs with a role in gene regulation and in human diseases. Mol. Biol. Rep. 41, 225–232. doi:http://dx.doi.org/10.1007/s11033-013-2855-1.
Vašák, M., Meloni, G., 2011. Chemistry and biology of mammalian metallothioneins. J. Biol. Inorg. Chem. 16, 1067–1078. doi:http://dx.doi.org/10.1007/s00775-011-0799-2.
Vendrell, J., Querol, E., Avilés, F.X., 2000. Metallocarboxypeptidases and their protein inhibitors. Structure, function and biomedical properties. Biochim. Biophys. Acta 28, 4–298. doi:http://dx.doi.org/10.1016/S0167-4838(99)00280-0.
Venkatesh, S., Workman, J.L., Smolle, M., 2013. UpSETing chromatin during non-coding RNA production. Epigenetics Chromatin 6, 16. doi:http://dx.doi.org/10.1186/1756-8935-6-16.
Walker, M.S., Hughes, T.A., 2008. Messenger RNA expression profiling using DNA microarray technology: diagnostic tool, scientific analysis or un-interpretable data? Int. J. Mol. Med. 21, 13–17. doi:http://dx.doi.org/10.3892/ijmm.21.1.13.
Wang, S.H., Lee, C.W., Chiou, A., Wei, P.K., 2010. Size-dependent endocytosis of gold nanoparticles studied by three-dimensional mapping of plasmonic scattering images. J. Nanobiotechnol. 8, 33. doi:http://dx.doi.org/10.1186/1477-3155-8-33.
Wingler, K., Böcher, M., Flohé, L., Kollmus, H., Brigelius-Flohé, R., 1999. mRNA stability and selenocysteine insertion sequence efficiency rank gastrointestinal glutathione peroxidase high in the hierarchy of selenoproteins. Eur. J. Biochem. 259, 149–157. doi:http://dx.doi.org/10.1046/j.1432-1327.19999.00012.x.
Wittmaack, K., 2011. Excessive delivery of nanostructured matter to submersed cells caused by rapid gravitational settling. ACS Nano 5, 3766–3778. doi:http://dx.doi.org/10.1021/nn200112u.
Yang, Y., Qu, Y., Lü, X., 2010. Global gene expression analysis of the effects of gold nanoparticles on human dermal fibroblasts. J. Biomed. Nanotechnol. 6, 234–246. doi:http://dx.doi.org/10.1166/jbn.2010.1128.
Zhang, Y., Yuan, F., Wu, X., Wang, M., Rechkoblit, O., Taylor, J.S., Geacintov, N.E., Wang, Z., 2000. Error-free and error-prone lesion bypass by human DNA polymerase kappa in vitro. Nucleic Acids Res. 28, 4138–4146.
Zhang, S.L., Tang, Y.P., Wang, T., Yang, J., Rao, K., Zhao, L.Y., Zhu, W.Z., Meng, X.H., Wang, S.G., Liu, J.H., et al., 2011. Clinical assessment and genomic landscape of a consanguineous family with three Kallmann syndrome descendants. Asian J. Androl. 13, 166–171. doi:http://dx.doi.org/10.1038/aja.2010.83.